BIOCHEMISTRY
including biophysical chemistry & molecular biology

Article

pubs.acs.org/biochemistry

The FKBP-Type Domain of the Human Aryl Hydrocarbon Receptor-Interacting Protein Reveals an Unusual Hsp90 Interaction

Miriam Linnert,[†,§] Yi-Jan Lin,[‡,§] Annika Manns,[†] Katja Haupt,[†] Anne-Katrin Paschke,[†] Gunter Fischer,[†] Matthias Weiwad,*[,†] and Christian Lücke*[,†]

[†]Max Planck Research Unit for Enzymology of Protein Folding, Weinbergweg 22, 06120 Halle (Saale), Germany

[‡]Graduate Institute of Natural Products and Center of Excellence for Environmental Medicine, Kaohsiung Medical University, Kaohsiung 807, Taiwan

Supporting Information

ABSTRACT: The aryl hydrocarbon receptor-interacting protein (AIP) has been predicted to consist of an N-terminal FKBP-type peptidyl-prolyl *cis/trans* isomerase (PPIase) domain and a C-terminal tetratricopeptide repeat (TPR) domain, as typically found in FK506-binding immunophilins. AIP, however, exhibited no inherent FK506 binding or PPIase activity. Alignment with the prototypic FKBP12 showed a high sequence homology but indicated inconsistencies with regard to the secondary structure prediction derived from chemical shift analysis of AIP$^{2-166}$. NMR-based structure determination of AIP$^{2-166}$ now revealed a typical FKBP fold with five antiparallel β-strands forming a half β-barrel wrapped around a central α-helix, thus permitting AIP to be also named FKBP37.7 according to FKBP nomenclature. This PPIase domain, however, features two structure elements that are unusual for FKBPs: (i) an N-terminal α-helix, which additionally stabilizes the domain, and (ii) a rather long insert, which connects the last two β-strands and covers the putative active site. Diminution of the latter insert did not generate PPIase activity or FK506 binding capability, indicating that the lack of catalytic activity in AIP is the result of structural differences within the PPIase domain. Compared to active FKBPs, a diverging conformation of the loop connecting β-strand C′ and the central α-helix apparently is responsible for this inherent lack of catalytic activity in AIP. Moreover, Hsp90 was identified as potential physiological interaction partner of AIP, which revealed binding contacts not only at the TPR domain but uncommonly also at the PPIase domain.

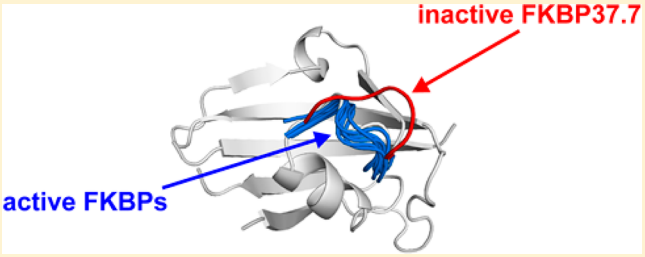

The 330 amino acid residues comprising aryl hydrocarbon receptor-interacting protein (AIP) has been discussed previously as a possible member of the FK506-binding protein (FKBP) superfamily.[1,2] On the basis of sequence comparison, AIP can be divided into a putative FKBP-type PPIase domain at the N-terminal end and a putative tetratricopeptide repeat (TPR) domain at the C-terminal end. However, no structural data from any AIP are available to date, except for the crystal structure of the TPR domain belonging to the AIP homologue from *Caenorhabditis elegans* (PDB ID code 3RKV). This TPR domain comprises three TPR motifs, as known from other TPR-containing FKBPs like FKB51 and FKBP52, for example.[3,4]

FKBPs belong to the enzyme class of peptidyl prolyl *cis/trans* isomerases (PPIases; E.C. 5.2.1.8) that assist the *cis/trans* interconversion of Xaa-Pro peptide bonds.[5] They generally comprise one or more N-terminal FKBP-type PPIase domain(s).[6] In addition, multidomain FKBPs feature also other functional regions at the C-terminal end, such as TPR domains, calmodulin binding domains, EF-hand motifs, or signal sequences. Presently, 16 proteins are considered to be members of the human FKBP family, and they are predominantly located in the cytosol or in the endoplasmatic reticulum.[7] However, not all of these FKBPs are active PPIases; currently only six members are confirmed to be active.[8] Hence, the assignment to the FKBP family is based not on catalytic activity but rather on sequence homology of the PPIase domains, while the true biological functions of the inherently inactive FKBPs often remains unknown.

To investigate the function of AIP, nonviable knockout mice were generated,[9] which displayed decreased blood flow to head and limb as well as heavy cardiovascular defects. Furthermore, missense mutations in the AIP gene or truncations of the protein seem to be related to pituitary tumor development.[10,11]

Because of the initial identification of the aryl hydrocarbon receptor (AhR) and the hepatitis B virus X protein as interaction partners, AIP is also referred to as AhR-associated protein (ARA9) or X-associated protein 2 (XAP2).[1,12,13] However, AIP has been identified as a binding partner for a plethora of other proteins, including several receptor proteins such as the estrogen receptor α (ERα), peroxisome proliferator-activated receptor α (PPARα), and the thyroid hormone receptor β1 (TRβ1), chaperone proteins such as Hsp90 and Hsc70, viral proteins, G-proteins, phosphodiesterases, and other proteins.[14]

The best investigated interaction of AIP is in the AhR complex. This heterotetrameric receptor complex is (i) composed of an

Received: December 11, 2012
Revised: February 15, 2013
Published: February 18, 2013

dx.doi.org/10.1021/bi301649m | *Biochemistry* 2013, 52, 2097−2107

AhR monomer, an AIP monomer, and an Hsp90 dimer and (ii) in the absence of any ligand located in the cytosol.[15,16] After binding of substances such as 2,3,7,8-tetrachlorodibenzo-*p*-dioxin (TCDD), the receptor complex translocates into the nucleus, where AIP and Hsp90 dissociate from AhR and the receptor dimerizes with the AhR nuclear translocator.[17] This newly formed dimeric receptor complex binds to a *xenobiotic response element* on the DNA, thus initiating the transcription of target genes such as cytochrome P-4501A1.[18] The same complex formation can be also observed in another heterotetrameric receptor complex with PPARα, whereby AIP and Hsp90 can distinguish between the receptor subtypes PPARα, PPARβ, and PPARγ.[19]

Moreover, an interaction between AIP and Hsp90 has been observed also in the absence of any receptor, although clearly weaker in this case.[1,20] This receptor-free AIP-Hsp90 interaction is similar to that of other TPR-containing proteins like FKBP52, for example,[21] since it occurs mainly between residues of the TPR motifs in AIP and the MEEVD motif at the C-terminal end of Hsp90.[4] However, additional interaction sites located at the C-terminus of AIP outside the TPR motifs were also noticed. Remarkably, destabilizing effects were observed even when merely parts of the PPIase domain were removed from AIP,[22,23] suggesting a possible role of the N-terminal AIP domain in this interaction.

Based on sequence homology, AIP had been predicted to represent a member of the FKBP family, although neither FK506 binding nor PPIase activity were reported to date.[24,25] Resonance assignments and subsequent chemical shift index analysis of the N-terminal AIP domain, however, have indicated a disagreement between the sequence alignment of AIP with FKBP12 and the NMR-derived arrangement of secondary structure elements, thus raising the question whether AIP in fact features a true FKBP fold.[26] Here we present the solution structure of AIP$^{2-166}$ together with an assessment of the lack of PPIase activity and FK506 binding, clearly demonstrating that AIP is a multidomain FKBP and elucidating the reason why it is catalytically inactive. Moreover, chaperone activity assays and ligand binding analyses with Hsp90 have been performed. We report that the chaperone activity is mediated by the TPR domain like in FKBP51 and not by the PPIase domain as for example in Sly D from *E. coli*.[27,28] Furthermore, we demonstrate that besides the already known TPR-mediated interaction between Hsp90 and AIP an additional unique interaction occurs between Hsp90 and the PPIase domain of AIP.

MATERIALS AND METHODS

Protein Preparation. Except where indicated otherwise, soluble recombinantly expressed human proteins were generally produced by using a pET30a vector (Novagen) in *E. coli* BL21(DE3) cells (Stratagene) that were grown in either 2YT medium (for nonlabeled protein) or M9 minimal medium (for isotope-labeled protein) at 37 °C, induced with 0.5 mM isopropyl β-D-thiogalactopyranoside (IPTG), harvested after 4 h, lysed by French press, and centrifuged at 100000*g* for 45 min. Thus produced proteins were generally purified with an EMD-DEAE-650(M) anion-exchange column (Merck) followed by a HiLoad Superdex 75 HR 16/60 size-exclusion column (GE Healthcare).

FKBP12 was produced and purified as previously described.[34,35]

Schistosoma japonicum GST was expressed using a pGEX-4T-1 vector (GE Healthcare). The cell lysate was purified using a Glutathione Sepharose 4B column (GE Healthcare).

AIP$^{2-330}$ expression was achieved at 30 °C. Following elution from the anion-exchange column using NaCl, the protein was precipitated with 30% $(NH_4)_2SO_4$ and subsequently centrifuged at 28000*g* for 30 min at 4 °C. The precipitated protein was redissolved, dialyzed against 25 mM Tris buffer (pH 7.2), and applied to a Q Sepharose anion-exchange column (GE Healthcare). The protein was finally purified by size-exclusion chromatography.

His$_6$-AIP$^{1-330}$ was cloned into a pET28a vector (Novagen). The protein was purified using a Ni-NTA affinity column (Qiagen), followed by anion-exchange and size-exclusion chromatography.

Nonlabeled and isotope-labeled AIP$^{2-166}$ samples were prepared as reported elsewhere.[26]

To obtain AIP$^{2-166\Delta100-144}$, the codons for amino acid residues 99 and 145 were linked via a nucleotide sequence encoding for Asp-Gly-Asp. Soluble protein was obtained 3 h after induction with IPTG at 30 °C. The protein was purified by anion-exchange and size-exclusion chromatography followed by another Q Sepharose anion-exchange column.

AIP$^{170-330}$ was generated at 30 °C. The protein was precipitated with 45% $(NH_4)_2SO_4$, redissolved after centrifugation, and purified using an EMD-Propyl-650(M) hydrophobic-interaction column, followed by anion-exchange and size-exclusion chromatography.

To produce GST−AIP$^{11-158}$, GST−AIP$^{1-166}$, GST−AIP$^{1-166\Delta100-144}$, GST−AIP$^{170-330}$, and GST−AIP$^{1-330}$ the corresponding coding sequences were cloned into the pGEX-5X-1 vector (GE Healthcare). Expression of GST−AIP$^{11-158}$ and GST−AIP$^{170-330}$ was achieved in *E. coli* DH5α cells (Novagene) grown at 30 °C in 2YT medium complemented with 5% glycerol. Expression of GST−AIP$^{1-166}$ and GST−AIP$^{1-166\Delta100-144}$ was performed in *E. coli* BL21(DE3) Rosetta cells (Novagene) that were grown at 30 °C in 2YT medium complemented with 5% glycerol and harvested 3 h after induction with 1 mM IPTG. All these GST variants were purified using a Glutathione Sepharose 4B column and subsequent size-exclusion chromatography. GST−AIP$^{1-330}$ was expressed in *E. coli* BL21-(DE3) Rosetta cells that were grown at 30 °C in 2YT medium complemented with 5% glycerol and harvested 3 h after induction. The protein was purified using Glutathione Sepharose 4B followed by anion-exchange and size-exclusion chromatography.

His$_6$-Hsp90β^{1-724}, His$_6$-Hsp90$\alpha^{628-732}$, and His$_6$-Hsp90$\beta^{620-724}$ were prepared using a pET28a vector in *E. coli* BL21(DE3) Rosetta cells, which were harvested 3 h after induction at 37 °C. Protein purification was carried out using a Ni-NTA affinity column, followed by anion-exchange and size-exclusion chromatography.

FLAG−AIP$^{1-330}$ was prepared by using a pCMV-Tag 2B vector (Stratagene) that had the coding sequence for FLAG−AIP$^{1-330}$ inserted. HEK293 cells were transfected with the manipulated vector by applying Lipofectamine 2000 (Invitrogen) and subsequently cultured for several weeks with increasing amounts of G418 until a stable FLAG−AIP$^{1-330}$ expressing cell line was obtained. For the preparation of cell lysate, the cells were resuspended in cell lysis buffer I, which consisted of MENG buffer (i.e., 25 mM MOPS, 2 mM EDTA, 0.02% sodium azide, 10% glycerol, pH 7.5), 10 mM Na_2MoO_4, 50 mM EDTA, 0.1% Nonidet P-40, 1.5 mM $MgCl_2$, protease inhibitor, benzonase, and phosphatase inhibitor and then lysed by sonication. Following centrifugation of the cell lysate for 15 min at 10000*g* and 4 °C, 25 mL of the supernatant with a protein concentration of 2 mg/mL protein was applied to 0.5 mL of anti-FLAG M2 affinity

agarose (Sigma-Aldrich). After removing unbound with 1 × TBS, the bound protein was eluted with 100−200 μg/mL FLAG peptide in 1 × TBS. As a control, the same procedure was also carried out with cells that were transfected with the non-manipulated pCMV−Tag 2B vector.

All human cell lines were purchased from DSZM (Braunschweig) and cultured as indicated by the distributor. The identities of the produced proteins were confirmed by mass spectrometry, revealing that the initial methionine of AIP had been removed after protein translation in all variants without an N-terminal tag. The structural integrity of the proteins was monitored by CD spectroscopy.

PPIase Activity Measurements. The PPIase activity was initially determined in the protease-coupled PPIase assay at 10 °C by using the peptide substrate succinyl-Ala-Phe-Pro-Phe-pNA, as previously described.[36] The PPIase activity of $AIP^{2-166\Delta100-144}$ was determined in the protease-free PPIase assay system by using the same peptide substrate, as described elsewhere.[37] Subsequently, to obtain a better signal-to-noise ratio in the protease-free PPIase assay, the PPIase activity of all other proteins was determined by using the substrate Abz-Ala-Phe-Pro-Phe-pNA, as recently reported.[29] All measurements were carried out using substrate concentrations well below K_M. Therefore, bimolecular rate constants (k_{cat}/K_M) could be calculated according to the equation $k_{cat}/K_M = (k_{obs} - k_{uncat})/[PPIase]$, where k_{uncat} is the first-order rate constant for uncatalyzed *cis*/*trans* isomerization, k_{obs} is the pseudo-first-order rate constant for *cis*/*trans* isomerization in the presence of enzyme, and [PPIase] represents the enzyme concentration.

Refolding of RNase T1. To investigate the refolding of RNase T1, a reduced and carboxymethylated S54G/P55N variant (RCM-T1) with only one *cis* proline, as reported elsewhere,[38] was employed. Unfolded RCM-T1 was stored in Tris buffer (100 mM, pH 8.0). The refolding was started by 50-fold dilution of RCM-T1 to a final concentration of 3.4 μM in high-salt Tris buffer (100 mM, 2 M NaCl, pH 8.0). The refolding reactions were monitored via the increase of fluorescence at 320 nm (excitation wavelength 268 nm) over a period of 45 min at 10 °C. The bimolecular rate constants (k_{cat}/K_M) were determined as described above.

Chaperone Activity Measurements. Thermal aggregation of citrate synthase was determined as described elsewhere.[39] Light scattering was measured during the aggregation reaction of 0.15 μM citrate synthase both with and without AIP variants for 20 min in 40 mM Hepes buffer (pH 7.5) at 43 °C. Thereby, the aggregation was monitored at the excitation and emission wavelength of 360 nm using a Hitachi F-3010 fluorescence spectrophotometer.

FK506 Binding Assay. To investigate binding of authentic AIP to FK506, 50 μL of a FK506-affinity matrix and 2.5 mL cell lysate (5 mg/mL) were used. Cell lysates were prepared as described above for $FLAG\text{-}AIP^{1-330}$ by using cell lysis buffer II (1 × TBS, 1 mM EDTA, 0.1% Nonidet P-40, 2% glycerol, 1.5 mM $MgCl_2$, protease inhibitor, benzonase, phosphatase inhibitor). In the experiments with purified FKBP12 or AIP, 20 μL of FK506-affinity matrix were incubated with 20 μg of purified protein in 30 μL of Tris-HCl buffer (20 mM, 100 mM NaCl, pH 7.5). After incubation for 1 h at 4 °C under moderate shaking, unbound protein was removed and the matrix was washed six times with 1 mL of the same buffer. To elute bound protein from the affinity matrix, the beads were resuspended in SDS sample buffer (40 μL in case of recombinant proteins and 100 μL in case of cell lysates) and boiled for 5 min at 96 °C. Proteins were subsequently separated by SDS polyacrylamide gel electrophoresis (SDS-PAGE) using 15−17.5% SDS gels. The same protocol was used for incubation of the control matrix.

GST Pull-down Assay. To investigate the binding of authentic Hsp90 to AIP, 80 μg GST or GST-AIP variants were immobilized by addition to 50 μL of GSH Sepharose for 2 h at 4 °C and afterward washed with MENG buffer and 10 mM Na_2MoO_4. Next, each sample was incubated overnight at 4 °C under moderate shaking with 1 mL of cell lysate (2.5 mg/mL), which was prepared as described above for $FLAG\text{-}AIP^{1-330}$. To subsequently remove unbound protein, the resin was washed three times with MENG buffer and 10 mM Na_2MoO_4. Bound protein was eluted for 10 min at room temperature with 40 μL of reduced glutathione (10 mM) in 25 mM Tris buffer (pH 7.5).

To investigate the binding of purified Hsp90 to AIP, 40 μg of GST or GST-AIP variants were immobilized by addition to 50 μL of GSH Sepharose for 1 h at 4 °C. Next, the GSH Sepharose was washed with 1 × PBS and incubated with 10 μg of purified protein for 1 h at 4 °C. Unbound protein was removed by washing three times with 1 × PBS, 1 × PBS with 0.1% Nonidet P-40, and 1 × PBS with 200 mM NaCl. Bound protein was eluted for 10 min at room temperature with 30 μL of reduced glutathione (10 mM) in 25 mM Tris buffer (pH 7.5).

NMR Spectroscopy. NMR data were collected as previously described.[26] For structure determination, the AIP^{2-166} concentration in each sample was set to 2 mM. NOE-based distance restraints for structure calculation were obtained from 2D homonuclear NOESY, 3D ^{15}N-edited NOESY-HSQC, and 3D ^{13}C-edited NOESY-HSQC spectra that were collected with 120 ms mixing time each at a Bruker Avance III 800 spectrometer operating at 800.23 MHz with 5 mm TCI cryoprobe. $^{1}H/^{15}N$-HSQC experiments for chemical shift perturbation (CSP) analysis were performed on a Bruker DRX 500 spectrometer operating at 500.13 MHz with a 5 mm TXI probe featuring gradient capability. All spectra were collected with the carrier placed on the water resonance, which was suppressed by a WATERGATE sequence. The NMR spectra were processed on a Silicon Graphics O2 workstation using the XWINNMR 3.5 software package at the DRX 500 spectrometer or TopSpin 2.1 at the Avance 800 spectrometer (both Bruker). A 90° phase-shifted squared sine-bell function was used for apodization in all dimensions. After Fourier transform, a polynomial baseline correction was applied to the processed spectra in the directly detected ^{1}H dimension. All chemical shifts were referenced to external 2,2-dimethyl-2-silapentane-5-sulfonate (DSS) in order to ensure consistency among the spectra.[40]

A combination of calculations with CYANA 3.0 (L. A. Systems) and DYANA 1.5 was applied to determine the three-dimensional structure of AIP^{2-166}. First, an automatic NOE assignment within seven cycles of structure calculation[41] was performed with CYANA, resulting in an ensemble of 20 conformers and generation of an NOE peak list in the final cycle. Based on the structural statistics, the NOE assignments were subsequently modified manually to further refine the structure using DYANA.[42] Stereospecific assignments for prochiral groups were obtained with GLOMSA.[43] The 20 best DYANA conformers were finally subjected to restrained energy minimization calculations using a distance-dependent dielectric model to mimic the presence of water, as previously described.[44]

For CSP analysis of the AIP/Hsp90 complexes, 0.6 mM AIP^{2-166} samples were employed with ligand concentrations set to 1.52 mM in the case of $His_6\text{-}Hsp90\beta^{620-724}$ and 1.02 mM in case of $His_6\text{-}Hsp90\beta^{1-724}$. Peak picking of backbone amide resonances

dx.doi.org/10.1021/bi301649m | *Biochemistry* 2013, 52, 2097−2107

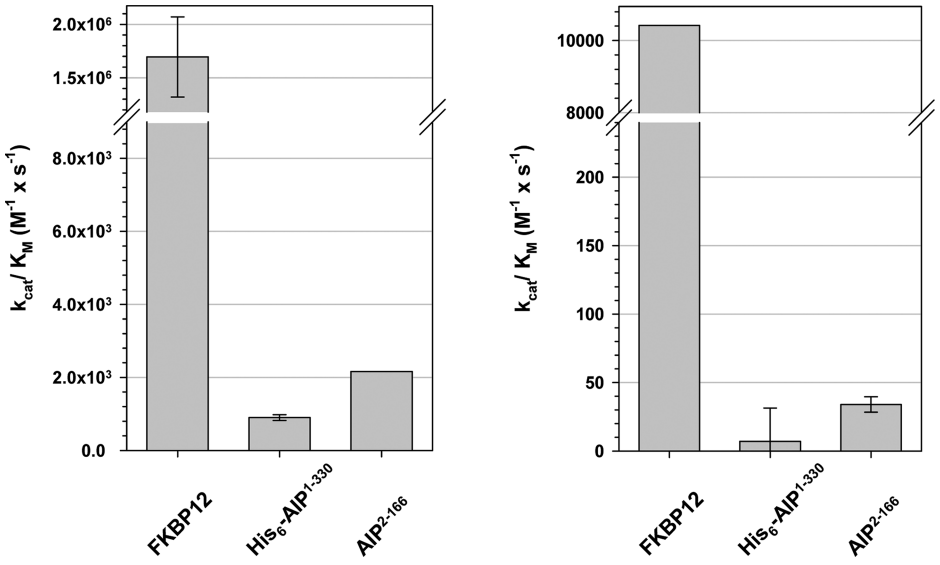

Figure 1. PPIase activity of AIP. The activity was measured in a protease-free PPIase assay (left) and during refolding of RCM-T1 (right). FKBP12 showed activity values that correspond to the known literature, whereas neither the PPIase domain of AIP (AIP^{2-166}) nor the full-length protein (His_6-AIP^{1-330}) revealed any significant activity.

was performed with the program FELIX 2000 (Accelrys Inc.). Chemical shift differences in the amide proton ($\Delta\delta_{1HN}$) and nitrogen ($\Delta\delta_{15N}$) resonances of the free and complexed protein forms were combined for each residue by using the expression $[(\Delta\delta_{1HN})^2 + (\Delta\delta_{15N}/6.5)^2]^{1/2}$.[45]

RESULTS AND DISCUSSION

Investigation of PPIase Activity and FK506 Binding. On the basis of sequence homology, AIP has been predicted to represent a member of the FKBP superfamily.[2] As a consequence, we aimed to investigate AIP with respect to PPIase activity and FK506 binding, two principal properties of active FKBP-type PPIase domains. To this end, we performed PPIase activity and FK506 binding assays both with full-length AIP (AIP^{2-330}) as well as its N-terminal domain (AIP^{2-166}). As a control, identical experiments were carried out with the prototypic FKBP12 for direct comparison.

First, the PPIase activity of AIP was determined using a protease-coupled PPIase assay. As no activity could be observed at all, the stability of AIP during the duration of the PPIase activity measurements was tested. Samples from these measurements were therefore analyzed in SDS polyacrylamide gels. It was observed that AIP had degraded entirely during the reaction time (Figure S1, Supporting Information). As a consequence, from here on all PPIase activity measurements were performed in a protease-free assay. Under these conditions (Figure 1), FKBP12 revealed a PPIase activity as known from literature,[29] i.e., $k_{kat}/K_M = 1.7 \times 10^6\ M^{-1}\ s^{-1}$, whereas AIP^{2-166} and AIP^{2-330} again showed nearly no activity with $k_{kat}/K_M = 0.9 \times 10^3$ and $2.2 \times 10^3\ M^{-1}\ s^{-1}$, respectively. To exclude that this lack of PPIase activity is due to the peptide substrate applied during the measurements, we checked PPIase activity also by employing RCM-T1 as protein substrate. FKBP12 again displayed an activity as known from literature,[30] i.e., $k_{kat}/K_M = 1.0 \times 10^4\ M^{-1}\ s^{-1}$, whereas AIP^{2-166} and AIP^{2-330} showed no activity (k_{kat}/K_M = 7 and 34 $M^{-1}\ s^{-1}$, respectively).

To exclude that post-translational modifications of eukaryotes influence the PPIase activity measurements, we furthermore produced FLAG-AIP^{1-330} in human HEK293 cells and purified the protein from the lysate. Again, measurements with this AIP derived from a human cell line showed PPIase activity neither with the peptide substrate nor with RCM-T1 (Figure S2, Supporting Information). Hence, it can be concluded that native AIP exhibits no PPIase activity.

Besides the PPIase activity, also FK506 binding to either the N-terminal domain or full-length AIP was investigated (Figure 2), using FKBP12 again as a control. While FKBP12 was bound nearly completely and specific to the FK506-affinity matrix, recombinant AIP^{2-166} did not bind at all. Moreover, the binding of authentic full-length AIP derived from several different human cell lines was investigated; however, while AIP was found both in the input and the unbound fractions, again no binding to FK506 could be detected. Hence, these results suggest that the putative FKBP domain of AIP is inherently inactive.

Three-Dimensional Structure of AIP^{2-166}. At this point, the reason for the lack of FKBP-typical functional properties was difficult to assess, since the sequence alignment between AIP and FKBP12 was inconsistent with the NMR-derived secondary structure prediction based on chemical shift index analysis.[26] Therefore, a comparison of key residues in the putative active site was not feasible, as the position of β-strand D for example remained unclear. To shed more light on the true nature of the N-terminal AIP domain, we determined the three-dimensional structure of AIP^{2-166} based on our previously reported resonance assignments.[26] The structural statistics of the final structure ensemble are presented in Table 1 and the structure coordinates have been deposited at the RCSB database under PDB ID code 2LKN.

The AIP^{2-166} structure (Figure 3) features a half β-barrel comprised of five antiparallel β-strands arranged in +3, +1, −3, +1 topology that wrap around a central α-helix, as is typical for a FKBP-type fold: i.e., strands βA (Ile13-Glu20), βB (Thr32-His42), βC (Thr48-Ile64), βD (Glu84-Asp91), βE (Asn144-Pro160), and central helix αII (Pro71-Thr79). Strands βA, βC and βE feature β-bulges at residues Ile18, Leu50 and Leu155, respectively. Moreover, strand βC is divided into two segments (Thr48-Asp52 and Lys58-Ile64) by a loop containing the short helix αI (Ser53-Arg56).

dx.doi.org/10.1021/bi301649m | *Biochemistry* 2013, 52, 2097−2107

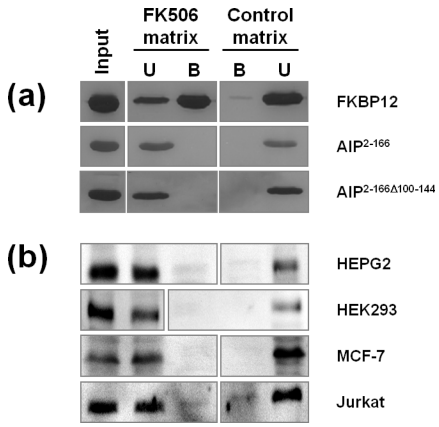

Figure 2. FK506 binding to AIP. (A) Recombinantly produced FKBP12, AIP$^{2-166}$, and AIP$^{2-166\Delta100-144}$ were incubated for 1 h with either the FK506-affinity matrix or the control matrix. Unbound protein (U) was subsequently removed and bound protein (B) eluted from the matrices. All samples were separated by SDS-PAGE and finally stained with silver nitrate. (B) The FK506-affinity matrix and the control matrix were incubated for 1 h with lysates from different human cells. Next, unbound protein (U) was removed and bound protein (B) subsequently eluted from the matrices. All samples were separated by SDS-PAGE. The proteins were transferred to a nitrocellulose membrane and AIP was stained with an AIP antibody.

Table 1. Structural Statistics of the 20 Selected Conformers of AIP$^{2-166}$ after Energy Minimization

structural statistics	
total no. of residues	165
total no. of distance restraints	3678
intraresidual	577
sequential ($\|i-j\|=1$)	987
medium range ($1<\|i-j\|\leq 4$)	724
long range ($\|i-j\|>4$)	1390
total no. of restraint violations >0.3 Å	1
total no. of restraint violations >0.2 Å	15
max restraint violation (Å)	0.33
Ramachandran plot statistics (%)	
residues in most favored regions	77.6[a] (82.1)[b]
residues in additionally allowed regions	19.8 (17.1)
residues in generously allowed regions	1.5 (0.7)
residues in disallowed regions	1.1 (0.2)
structural precision (Å)	
backbone atom[c] RMSD (residues 3−110, 136−165)	0.75 ± 0.14
heavy atom RMSD (residues 3−110, 136−165)	1.44 ± 0.15

[a]AIP residues 2−166. [b]AIP residues 2−110 and 136−166. [c]N, C$^{\alpha}$, C′ and O.

Based on these structural features, i.e., an N-terminal PPIase domain and a C-terminal TPR domain, AIP may thus be also referred to as FKBP37.7 according to the nomenclature criteria of the FKBP superfamily.[2,31] However, the N-terminal AIP domain furthermore features two structure elements that are atypical for FKBPs:

(1) The N-terminal helix α0, which spans from Ile4 to Asp11 and precedes strand βA of the PPIase domain, is highly unusual and its arrangement relative to the FKBP domain unique within the FKBP superfamily. An additional β-strand that extends the antiparallel β-sheet at the N-terminus is known for several active (FKBP35 and the first domain of both FKBP51 and FKBP52) and inactive (FKBP36, FKBP38 and FKBP42, each second

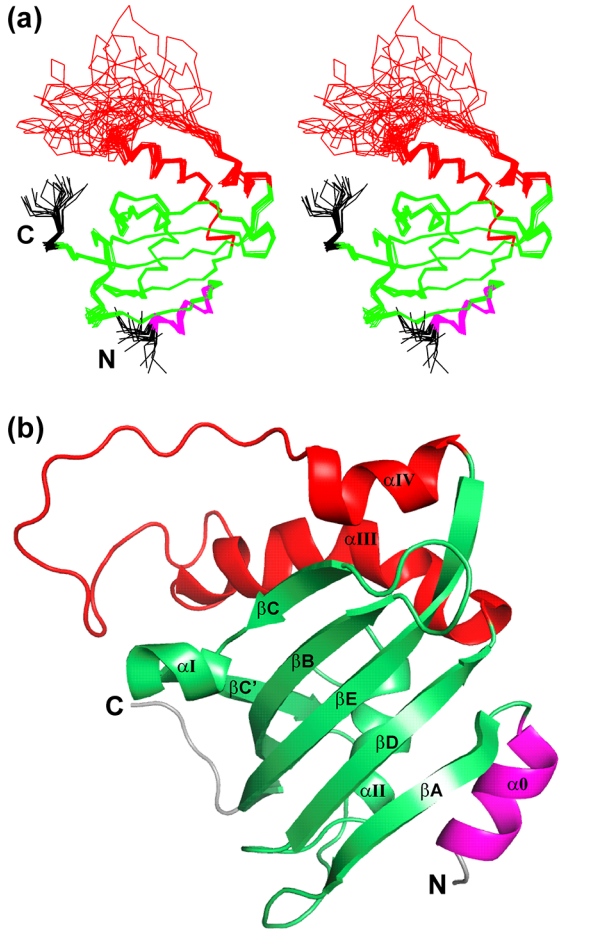

Figure 3. Solution structure of AIP$^{2-166}$. (A) Stereoplot of the superposed Cα traces of the 20 selected AIP$^{2-166}$ conformers. The FKBP-type PPIase domain is shown in green. The additional N-terminal helix α0 is colored magenta. The linker between the last two β-strands, i.e., the βD-βE extension including helices αIII and αIV, is displayed in red. The N and C termini are labeled. (B) Cartoon of the representative AIP$^{2-166}$ conformer with the secondary structure elements labeled. The same color code as in panel A is used.

domain of FKBP51, FKBP52, and FKBP73, as well as the third domain of FKBP73) PPIase domains. FKBP36 and the first domain of FKBP51 moreover feature an N-terminal helix that runs across the outside face of the β-sheet nearly orthogonal to the β-strands. An α-helix such as α0 in AIP, however, which is oriented nearly parallel to the first strand βA and thus appears like an N-terminal extension of the antiparallel β-sheet, is unique to all presently known PPIase domain structures. Deletion of helix α0 from the N-terminus furthermore resulted in a considerably reduced stability of AIP, as the variant lacking helix α0 (GST-AIP$^{11-158}$) exhibited a markedly reduced yield of soluble protein during overexpression in *E. coli* and became more rapidly degraded during protein preparation and purification compared to GST−AIP$^{1-166}$, as indicated by the results described below. A similar observation was reported by Meyer et al.,[16] who noticed an increased expression level of AIP$^{1-330}$−FLAG compared to AIP$^{17-330}$−FLAG and therefore suggested that this may be due to a higher turnover of AIP$^{17-330}$−FLAG in cells. The increased AIP$^{1-166}$ stability due to helix α0 can most likely be attributed to its contacts with both strand βA and helix αII, thereby partially covering the central helix inside the half β-barrel (Figure S3, Supporting Information).

dx.doi.org/10.1021/bi301649m | *Biochemistry* 2013, 52, 2097−2107

Figure 4. (A) Superposition of the PPIase domains of AIP$^{2-166}$ (black) and FKBP12 (white; PDB ID code 2PPN). This molecule orientation shows the view into the putative active site. AIP$^{2-166}$ is presented without N-terminal helix α0 and βD-βE extension. (B) Sequence alignment between FKBP12 and AIP$^{1-166}$ based on sequence and structure homologies. Highlighted by white and gray boxes are strand and helix elements of FKBP12, respectively, according to the FKBP12 crystal structure (PDB ID code 2PPN) and the AIP$^{2-166}$ solution structure. Key residues for FK506 binding are shown in bold type.

(2) The helices αIII (Ile92-Val110) and αIV (A136-Gln143) represent the start and end of an unusually long insert that connects the last two strands βD and βE of the FKBP-type PPIase domain. All FKBPs possess an insert of approximately 20 residues at this position, which generally starts with a short helical loop and may contain additional short secondary structure elements. In AIP$^{2-166}$, on the other hand, the insert encompasses 57 amino acid residues (Figure S3, Supporting Information), beginning with a rather long helical segment that comprises 19 residues (αIII), followed by an apparently mostly random-coil structure, and ending with the FKBP-atypic α-helix (αIV). Sequence comparison suggests that this particular insert does not represent another TPR motif, for example as a result of gene splicing. From here on, we will refer to this unique structure element as the "βD-βE extension". This extension, in particular its two helical segments, covers the putative active site of the AIP PPIase domain. The nonstructured section of the βD-βE extension, i.e., residues Gly111−His135, includes the segment Arg119−Ser132, which features a large number of nonassigned residues,[26] suggesting that this region of AIP may exhibit pronounced amide proton exchange or conformational variability.

Comparison of the AIP$^{2-166}$ Structure with Inherently Active FKBPs. Although the three-dimensional fold of the N-terminal AIP domain is rather similar to FKBP12, as indicated by a total backbone RMSD of 1.97 Å (excluding the βD-βE extension), a few differences still exist: aside from the unique helix α0 and the much longer βD-βE extension mentioned above, the AIP$^{2-166}$ sequence diverges from FKBP12 in the segment connecting strands βA and βB (one residue longer in AIP) and the turn between strands βB and βC (two residues longer in AIP). Nevertheless, superposition of the N-terminal AIP domain with the prototypic FKBP12 (Figure 4A) showed a very similar FKBP-type fold with a backbone root-mean-square deviation (RMSD) of 1.28 Å for the secondary structure elements. Hence, the previously reported chemical shift index analysis[26] had produced the correct secondary structure arrangement in contrast to the ClustalW2 prediction. The correct sequence alignment, based on ClustalW2 and modified according to structure homology, is thus shown in Figure 4B. In view of this rather close agreement in the overall fold between AIP$^{2-166}$ and FKBP12, the reason(s) for the inherent lack of PPIase activity and FK506 binding capability in AIP seem to be associated to local details of the protein structure. We now discuss several factors that could potentially influence the FKBP-type functional properties of AIP.

One possible explanation for the apparent lack of FKBP-like functional characteristics could be that the βD-βE extension covers the putative active site in AIP$^{2-166}$. This structural arrangement may hinder potential ligands or substrates to access the putative active site. In order to further investigate this possibility, a shortened construct of the N-terminal AIP domain that lacks the βD-βE extension (i.e., AIP$^{2-166\Delta100-144}$) was generated. CD and NMR-based ^{1}H/^{15}N-HSQC spectra of AIP$^{2-166\Delta100-144}$ revealed that the structure of the PPIase domain remained intact. Still, despite the missing βD-βE extension this construct showed neither FK506 binding (Figure 2) nor PPIase activity. Even though a bimolecular rate constant of $k_{kat}/K_M \sim 5 \times 10^4$ M^{-1} s^{-1} was determined in both the protease-coupled and the protease-free PPIase assay, this apparent small activity could be reduced by more than 95% upon addition of 50 μM [*O*-carboxymethyl-D-Ser^{8}]-CsA, whereas FK506 had no effect on the PPIase activity.[32] The same observation was made in the assay using the protein substrate RCM-T1. Hence, the measured PPIase activity most likely is due to contamination with cyclophilin impurities and not to AIP$^{2-166\Delta100-144}$. Moreover, neither AIP$^{2-166}$ nor AIP$^{2-166\Delta100-144}$ showed chaperone activity, indicating that the βD-βE extension is not a chaperone domain, like for example in *E. coli* SlyD.[33] Hence, the chaperone activity found in AIP relates to only the TPR domain (Figure 5), as is also the case for the TPR-containing FKBP52.[27]

An alternative explanation for the inherent lack of FKBP-like functional properties in AIP could be the replacement or reorientation of key residues in the putative active site. FK506 is bound to FKBP12 via four hydrogen bonds (Figure S4, Supporting Information) in addition to several hydrophobic contacts with residues lining the binding pocket. Comparison of these key residues in FKBP12 and AIP$^{2-166}$ revealed a fairly high degree of conservation in both hydrophobicity and position of the corresponding side-chains (Figure S5A, Supporting Information), except for the residues located in the loop that connects strand βC′ and helix αII. In all inherently active FKBP-type PPIase domains this latter loop consist of 7 fairly conserved residues (Table S1, Supporting Information), whereby the last three residues are characterized by a motif that consists of a hydrophilic amino acid (glutamate, glutamine, or lysine) followed by valine and isoleucine. In the case of FKBP12, this motif is defined by residues E54, V55, and I56, which are replaced in AIP by F68, K69, and L70, respectively. In principle, hydrophobic binding contacts to the ligand via side chains, which occur at residues I56 and V55 in the FKBP12 loop, could be envisioned also for the corresponding AIP residues L70 and the aliphatic part of K69. Furthermore, hydrogen bonding to

dx.doi.org/10.1021/bi301649m | *Biochemistry* 2013, 52, 2097−2107

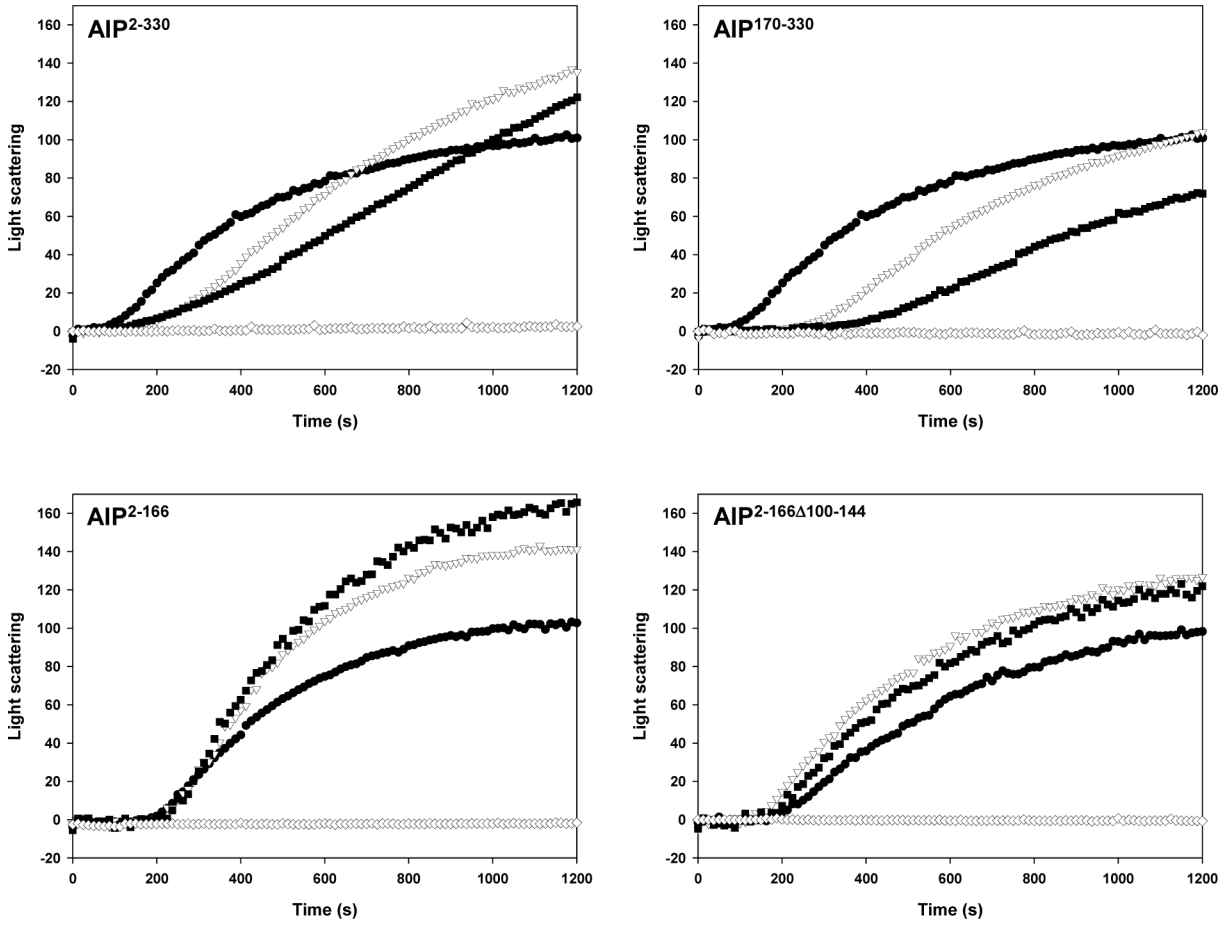

Figure 5. Chaperone activity of AIP during the thermal aggregation of citrate synthase. The turbidity of the solution at 360 nm and 43 °C was measured for 20 min as light scattering (in arbitrary units). Aggregation of 0.15 μM citrate synthase was monitored in the absence of additional protein (●), in the presence of 0.5 μM AIP (▽), and in the presence of 1.5 μM AIP (■). As a control, the aggregation of AIP^{2-166} (0.5 μM), $AIP^{2-166\Delta100-144}$ (0.5 μM), AIP^{2-330} (1.5 μM), and $AIP^{170-330}$ (1.5 μM) was determined in the absence of citrate synthase (◊).

FK506 via backbone atoms only, as is the case for E54 in FKBP12, should be possible also for F68 in AIP as long as the loop conformation is not altered. The three-dimensional structure of AIP^{2-166}, however, indicates that precisely the substitutions E54 (FKBP12) to F68 (AIP) and V55 (FKBP12) to K69 (AIP) seem to have a drastic effect on the conformation of the loop between strand βC′ and the central helix αII (Figure S5B, Supporting Information), such that the atoms F68 O and L70 N, which are crucial for hydrogen bonding with the FK506 ligand, are strongly displaced from their respective locations in FKBP12. As a consequence, the conformation of this loop diverges considerably from that found in the active FKBP domains (Figure 6), thereby also causing a slight tilt of the central helix αII (Figure 4A). As reported recently,[31] the inherently inactive FKBP-type PPIase domains deviate significantly from the prototypic FKBP12 fold precisely in this loop (Figure S6, Supporting Information) [except maybe for the third PPIase domain of FKBP73, where the small hydrophobic alanine side-chain in the 3-residue motif (Table S1, Supporting Information) apparently does not compromise the loop structure but another key residue responsible for hydrogen-bond interaction with FK506 is modified]. Hence, in spite of several conservative replacements of key residues in the active site of FKBP12 (i.e., F36, F46, F48, I56, and I91 are replaced in AIP by L50, M60, L62, L70, and L141, respectively), it seems that in particular the substitutions of FKBP12 residues E54 and V55 by F68 and K69 in AIP are primarily responsible for the lack of activity

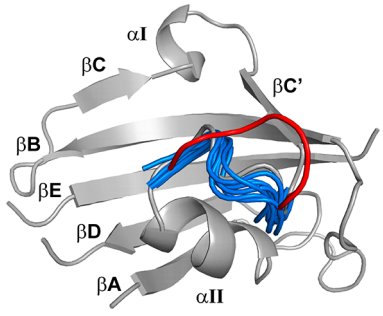

Figure 6. Superposition of the structures presently known for active PPIase domains (i.e., FKBP12, FKBP12.6, FKBP13, FKBP25, and FKBP35 as well as the first domains of FKBP51, FKBP52, and FKBP73) and the PPIase domain of AIP^{2-166}. The conformation of the loop between strand βC′ and the central helix αII is very similar to FKBP12 (gray cartoon; PDB ID code 2PPN) in all the active domains (blue ribbons) but diverges considerably in AIP (red ribbon). This figure is based on PDB entries 1C9H, 1KT0, 1PBK, 1Q1C, 2LKN, 2PBC, 2PPN, 2VN1, and 3JYM.

in the latter protein. While in FKBP12 the hydrophilic E54 side-chain extends to the protein surface and the hydrophobic V55 side-chain is part of the active site, the altered side-chain polarities and charges of the corresponding AIP residues F68 and K69 apparently cause a change in the loop conformation such that the F68 ring is buried in the hydrophobic active site and the K69 side-chain points

dx.doi.org/10.1021/bi301649m | *Biochemistry* 2013, 52, 2097−2107

toward the surface. We therefore postulate that the relative conformation of this particular loop between strand βC′ and helix αII is a crucial key to the catalytic function of FKBP-type PPIase domains. In order to verify this hypothesis, an extensive mutagenesis-based study would be required, which should selectively replace the seven loop residues either in FKBP12, to alter the loop structure and thus cause a loss of PPIase activity, or in AIP, to produce the correct loop conformation and thus generate PPIase activity.

The PPIase Domain of AIP Interacts with Hsp90. As AIP apparently does not show FKBP-typical functional characteristics, alternative properties of this protein may be envisioned. We therefore tested protein binding to AIP using pull-down experiments with human cell lysate (Figure 7A). Interestingly, while AhR was not found as AIP binding partner, one of the proteins that revealed binding both to full-length AIP and to the AIP PPIase domain alone was Hsp90. The interaction between full-length AIP and Hsp90 has been observed in an independent study also by Li and co-workers,[46] whereas the Hsp90 interaction with the N-terminal PPIase domain of AIP is unique within the FKBP family. Moreover, the binding of the AIP PPIase domain to Hsp90 was considerably weaker in case of AIP$^{2-166\Delta100-144}$, indicating that the exceptional βD-βE extension may be involved in the AIP−Hsp90 interaction.

Additional pull-down experiments with GST−AIP$^{11-158}$, GST−AIP$^{170-300}$, and GST−AIP$^{1-330}$ in the presence of the recombinantly produced and purified C-terminal domain of Hsp90 furthermore clearly revealed a direct interaction between the PPIase domain and Hsp90 (Figure S7, Supporting Information). As a consequence, it could be hypothesized that the interaction of Hsp90 with the βD-βE extension of AIP might render the putative active site to some extent accessible and thus the PPIase domain active, but such an influence of full-length Hsp90 on the PPIase activity of AIP was not detected.

Seven members of the PPIase enzyme class as well as many other proteins, e.g., PP5 and Hop, compete directly for a common TPR motif-acceptor site in Hsp90, resulting in the formation of distinct cochaperone−Hsp90−receptor complexes.[47] Additional Hsp90-binding sites apart from the TPR domain may thus represent a selection criterion for Hsp90 targeting. Accordingly, other PPIases harbor Hsp90-binding sites also beyond the TPR domain. Cyclophilin 40, for example, possesses an additional binding site in a part of the sequence that follows the PPIase domain, while in case of both FKBP51 and FKBP52 C-terminal segments located outside the TPR domain cause differential binding to Hsp90.[48−50] A catalytically active FKBP-type PPIase domain, however, seems not to be required for the Hsp90 interaction.

Although the affinity between AIP$^{2-166}$ and Hsp90 could not be determined by isothermal titration calorimetry, a previous report by Kazlauskas et al.[22] had also indicated a reduced interaction between Hsp90 and AIP if the PPIase domain or parts thereof were removed, further corroborating an involvement of the AIP PPIase domain in this interaction. As a consequence, we now performed CSP experiments with ^{15}N-labeled AIP$^{2-166}$ and nonlabeled Hsp90 to identify the binding interface on the AIP surface. Even though only very small CSP effects were observed, in agreement with a rather weak protein−protein interaction, significant line broadening occurred in the ^{1}H/^{15}N-HSQC spectra upon addition of full-length Hsp90 (Figure S8, Supporting Information), apparently due to an altered tumbling rate of AIP$^{2-166}$ in the transient high-molecular-weight complex. Interestingly, while line-broadening in the presence of full-length

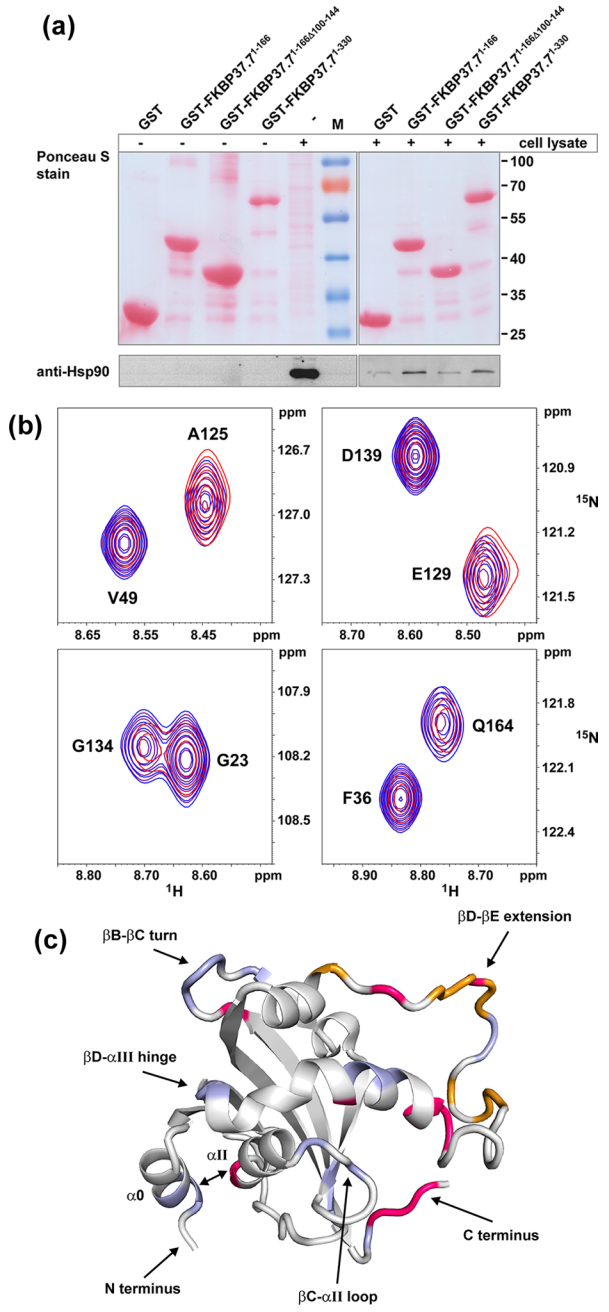

Figure 7. Binding of full-length Hsp90 to the PPIase domain of AIP. (A) GST, GST−AIP$^{1-166}$, GST−AIP$^{1-166\Delta100-144}$, and GST−AIP$^{1-330}$ were immobilized to GSH Sepharose and then incubated with HEK293 cell lysate. After removal of unbound protein, the bound protein was eluted with 10 mM reduced glutathione. All samples were applied to SDS-PAGE and the separated proteins subsequently transferred to a nitrocellulose membrane, where Hsp90 was stained with an Hsp90 antibody. (B) Overlay of sections from ^{1}H/^{15}N-HSQC spectra collected with 0.6 mM ^{15}N-labeled AIP$^{2-166}$ in the nonbound state (purple), in presence of 1.52 mM His$_6$-Hsp90$\beta^{620-724}$ (blue) and in presence of 1.02 mM His$_6$-Hsp90β^{1-724} (red). The signals of certain residues such as A125, E129, G134 (all βD-βE extension) and Q164 (C-terminus) show small but observable chemical shift changes in both complex states, which are always more pronounced in the presence of full-length Hsp90. (C) CSP mapping of AIP$^{2-166}$ residues affected by binding of His$_6$-Hsp90β^{1-724}. The most strongly affected residues (>0.008 ppm) are indicated in red, less affected residues (>0.006 ppm) in blue, and nonassigned residues belonging to the βD-βE extension in orange.

dx.doi.org/10.1021/bi301649m | *Biochemistry* 2013, 52, 2097−2107

Hsp90 was observed for signals belonging to AIP$^{2-166}$ residues located in the structured part of the AIP PPIase domain, the signal intensities of residues residing in the βD-βE extension or at the C-terminal end, where the most pronounced CSP effects could be found as discussed below, were not so much affected, thus indicating a high degree of mobility also in the presence of Hsp90.

The CSP effects detected in the presence of full-length Hsp90 (His$_6$-Hsp90β$^{1-724}$) as well as its C-terminal domain (His$_6$-Hsp90β$^{620-724}$) usually showed the same general trend, with signal displacements always a bit more pronounced when full-length Hsp90 was present (Figure 7B). Subsequent CSP mapping (Figure 7C) revealed that the AIP$^{2-166}$ residues showing the most pronounced signal shifts are located either in the βD−βE extension as well as adjacent structure elements (i.e., the βB−βC turn, the βC−αII loop and the βD−αIII hinge) or the C-terminal end of AIP$^{2-166}$. Moreover, the presumably secondary CSP effects observed at the interface between helices α0 and αII are a further indication of the stabilizing nature of the FKBP-atypical N-terminal helix.

Considering the fact that the nonstructured and apparently highly dynamic G111-H135 segment of the βD−βE extension contains a considerable number of residues that could not be assigned and which are interspersed with residues that are affected by Hsp90 binding, it seems very likely that a larger part of this unusual PPIase domain insert may be involved in the Hsp90 interaction (Figure 7C) than indicated by CSP analysis. The lack of AIP backbone amide signals belonging to the nonassigned residues in the βD−βE extension, which might additionally emerge in the ^{1}H/^{15}N-HSQC spectra when Hsp90 attaches to AIP$^{2-166}$, constitutes yet another indication that the interaction between Hsp90 and the PPIase domain of AIP is very weak and transient, which possibly explains why this interaction was not detected in former studies.

CONCLUSIONS

Based on the sequential and structural homologies between the AIP PPIase domain and FKBP12, AIP can be considered a true member of the FKBP superfamily and referred to as FKBP37.7, even though neither FK506 binding nor PPIase activity could be observed for this protein. The AIP$^{2-166}$ structure features several elements which are unique to FKBP-type PPIase domains, such as a stabilizing N-terminal α-helix (α0) and a rather long insert between strands βD and βE. Based on comparison with the structures of other active and inactive FKBP-type PPIase domains, a diverging conformation of the loop between strand βC′ and helix αII has been established as the most likely origin for the lack of PPIase activity in AIP. Moreover, Hsp90 was identified as an interaction partner of the AIP PPIase domain via pull-down and NMR-based CSP experiments, indicating that the unusually long and apparently highly dynamic βD-βE extension in AIP takes part in the AIP-Hsp90 interface, as is likely to occur for example also in the AhR/AIP/Hsp90$_2$ heterotetrameric receptor complex.

ASSOCIATED CONTENT

Supporting Information

Eight supplementary figures (S1−S8) showing SDS-PAGE, PPIase assay, and NMR data as well as structure comparisons and one supplementary table (S1) presenting a sequence comparison. This material is available free of charge via the Internet at http://pubs.acs.org.

Accession Codes

The structure coordinates of human AIP$^{2-166}$ have been deposited at the RCSB database under PDB ID code 2LKN.

AUTHOR INFORMATION

Corresponding Author

*Tel: +49-345-5522801. Fax: +49-345-5511972. E-mail: (M.W.) weiwad@enzyme-halle.mpg.de. (C.L.) luecke@enzyme-halle.mpg.de.

Author Contributions

§These authors contributed equally.

Funding

This work was supported by Grant Nos. BMBF 0315638B and 03IS2211H of the German Ministry for Research and Education.

Notes

The authors declare no competing financial interest.

ACKNOWLEDGMENTS

We are grateful to Prof. Jochen Balbach (University of Halle, Germany) for providing access to the 800 MHz NMR spectrometer. Monika Seidel (Max Planck Research Unit for Enzymology of Protein Folding) is acknowledged for excellent technical assistance.

ABBREVIATIONS

AhR, aryl hydrocarbon receptor; AIP, aryl hydrocarbon receptor-interacting protein; CSP, chemical shift perturbation; FKBP, FK506-binding protein; IPTG, isopropyl-β-D-thiogalactopyranoside; PPIase, peptidyl prolyl *cis/trans* isomerase; RCM-T1, reduced and carboxymethylated S54G/P55N variant of RNase T1; RMSD, root-mean-square deviation; SDS-PAGE, SDS polyacrylamide gel electrophoresis; TPR, tetratricopeptide repeat

REFERENCES

(1) Carver, L. A., and Bradfield, C. A. (1997) Ligand-dependent interaction of the aryl hydrocarbon receptor with a novel immunophilin homolog *in vivo*. *J. Biol. Chem. 272*, 11452−11456.

(2) Schiene-Fischer, C., and Yu, C. (2001) Receptor accessory folding helper enzymes: the functional role of peptidyl prolyl *cis/trans* isomerases. *FEBS Lett. 495*, 1−6.

(3) Sinars, C. R., Cheung-Flynn, J., Rimerman, R. A., Scammell, J. G., Smith, D. F., and Clardy, J. (2003) Structure of the large FK506-binding protein FKBP51, an Hsp90-binding protein and a component of steroid receptor complexes. *Proc. Natl. Acad. Sci. U.S.A. 100*, 868−873.

(4) Wu, B., Li, P., Liu, Y., Lou, Z., Ding, Y., Shu, C., Ye, S., Bartlam, M., Shen, B., and Rao, Z. (2004) 3D structure of human FK506-binding protein 52: implications for the assembly of the glucocorticoid receptor/Hsp90/immunophilin heterocomplex. *Proc. Natl. Acad. Sci. U.S.A. 101*, 8348−8353.

(5) Fischer, G., Bang, H., and Mech, C. (1984) Determination of enzymatic catalysis for the cis-trans-isomerization of peptide binding in proline-containing peptides. *Biomed. Biochim. Acta 43*, 1101−1111.

(6) Fischer, G., and Aumüller, T. (2003) Regulation of peptide bond *cis/trans* isomerization by enzyme catalysis and its implication in physiological processes. *Rev. Physiol. Biochem. Pharmacol. 148*, 105−150.

(7) Rulten, S. L., Hodder, E., Ripley, T. L., Stephens, D. N., and Mayne, L. V. (2008) Alcohol induces DNA damage and the Fanconi anemia D2 protein implicating FANCD2 in the DNA damage response pathways in brain. *Alcohol. Clin. Exp. Res. 32*, 1186−1196.

(8) Fanghänel, J., and Fischer, G. (2004) Insights into the catalytic mechanism of peptidyl prolyl *cis/trans* isomerases. *Front. Biosci. 9*, 3453−3478.

(9) Lin, B. C., Sullivan, R., Lee, Y., Moran, S., Glover, E., and Bradfield, C. A. (2007) Deletion of the aryl hydrocarbon receptor-associated protein 9 leads to cardiac malformation and embryonic lethality. *J. Biol. Chem. 282*, 35924−35932.
(10) Chahal, H. S., Chapple, J. P., Frohman, L. A., Grossman, A. B., and Korbonits, M. (2010) Clinical, genetic and molecular characterization of patients with familial isolated pituitary adenomas (FIPA). *Trends Endocrinol. Metab. 21*, 419−427.
(11) Georgitsi, M., Heliovaara, E., Paschke, R., Kumar, A. V., Tischkowitz, M., Vierimaa, O., Salmela, P., Sane, T., De Menis, E., Cannavo, S., Gundogdu, S., Lucassen, A., Izatt, L., Aylwin, S., Bano, G., Hodgson, S., Koch, C. A., Karhu, A., and Aaltonen, L. A. (2008) Large genomic deletions in AIP in pituitary adenoma predisposition. *J. Clin. Endocrinol. Metab. 93*, 4146−4151.
(12) Kuzhandaivelu, N., Cong, Y. S., Inouye, C., Yang, W. M., and Seto, E. (1996) XAP2, a novel hepatitis B virus X-associated protein that inhibits X transactivation. *Nucleic Acids Res. 24*, 4741−4750.
(13) Ma, Q., and Whitlock, J. P., Jr. (1997) A novel cytoplasmic protein that interacts with the Ah receptor, contains tetratricopeptide repeat motifs, and augments the transcriptional response to 2,3,7,8-tetrachlorodibenzo-p-dioxin. *J. Biol. Chem. 272*, 8878−8884.
(14) Trivellin, G., and Korbonits, M. (2011) AIP and its interacting partners. *J. Endocrinol. 210*, 137−155.
(15) Chen, H. S., and Perdew, G. H. (1994) Subunit composition of the heteromeric cytosolic aryl hydrocarbon receptor complex. *J. Biol. Chem. 269*, 27554−27558.
(16) Meyer, B. K., Pray-Grant, M. G., Vanden Heuvel, J. P., and Perdew, G. H. (1998) Hepatitis B virus X-associated protein 2 is a subunit of the unliganded aryl hydrocarbon receptor core complex and exhibits transcriptional enhancer activity. *Mol. Cell. Biol. 18*, 978−988.
(17) Petrulis, J. R., and Perdew, G. H. (2002) The role of chaperone proteins in the aryl hydrocarbon receptor core complex. *Chem. Biol. Interact. 141*, 25−40.
(18) Beischlag, T. V., Luis Morales, J., Hollingshead, B. D., and Perdew, G. H. (2008) The aryl hydrocarbon receptor complex and the control of gene expression. *Crit. Rev. Eukaryot. Gene Expr. 18*, 207−250.
(19) Sumanasekera, W. K., Tien, E. S., Turpey, R., Vanden Heuvel, J. P., and Perdew, G. H. (2003) Evidence that peroxisome proliferator-activated receptor α is complexed with the 90-kDa heat shock protein and the hepatitis virus B X-associated protein 2. *J. Biol. Chem. 278*, 4467−4473.
(20) Bell, D. R., and Poland, A. (2000) Binding of aryl hydrocarbon receptor (AhR) to AhR-interacting protein. The role of hsp90. *J. Biol. Chem. 275*, 36407−36414.
(21) Blatch, G. L., and Lassle, M. (1999) The tetratricopeptide repeat: a structural motif mediating protein-protein interactions. *BioEssays 21*, 932−939.
(22) Kazlauskas, A., Poellinger, L., and Pongratz, I. (2002) Two distinct regions of the immunophilin-like protein XAP2 regulate dioxin receptor function and interaction with hsp90. *J. Biol. Chem. 277*, 11795−11801.
(23) Meyer, B. K., and Perdew, G. H. (1999) Characterization of the AhR-hsp90-XAP2 core complex and the role of the immunophilin-related protein XAP2 in AhR stabilization. *Biochemistry 38*, 8907−8917.
(24) Carver, L. A., LaPres, J. J., Jain, S., Dunham, E. E., and Bradfield, C. A. (1998) Characterization of the Ah receptor-associated protein, ARA9. *J. Biol. Chem. 273*, 33580−33587.
(25) Laenger, A., Lang-Rollin, I., Kozany, C., Zschocke, J., Zimmermann, N., Rüegg, J., Holsboer, F., Hausch, F., and Rein, T. (2009) XAP2 inhibits glucocorticoid receptor activity in mammalian cells. *FEBS Lett. 583*, 1493−1498.
(26) Linnert, M., Haupt, K., Lin, Y.-J., Kissing, S., Paschke, A.-K., Fischer, G., Weiwad, M., and Lücke, C. (2012) NMR assignments of the FKBP-type PPIase domain of the human aryl-hydrocarbon receptor-interacting protein (AIP). *Biomol. NMR Assign. 6*, 209−212.
(27) Pirkl, F., Fischer, E., Modrow, S., and Buchner, J. (2001) Localization of the chaperone domain of FKBP52. *J. Biol. Chem. 276*, 37034−37041.
(28) Scholz, C., Eckert, B., Hagn, F., Schaarschmidt, P., Balbach, J., and Schmid, F. X. (2006) SlyD proteins from different species exhibit high prolyl isomerase and chaperone activities. *Biochemistry 45*, 20−33.
(29) Zoldák, G., Aumüller, T., Lücke, C., Hritz, J., Oostenbrink, C., Fischer, G., and Schmid, F. X. (2009) A library of fluorescent peptides for exploring the substrate specificities of prolyl isomerases. *Biochemistry 48*, 10423−10436.
(30) Scholz, C., Rahfeld, J., Fischer, G., and Schmid, F. X. (1997) Catalysis of protein folding by parvulin. *J. Mol. Biol. 273*, 752−762.
(31) Lücke, C., and Weiwad, M. (2011) Insights into immunophilin structure and function. *Curr. Med. Chem. 18*, 5333−5354.
(32) Zhang, Y., Erdmann, F., Baumgrass, R., Schutkowski, M., and Fischer, G. (2005) Unexpected side chain effects at residue 8 of cyclosporin A derivatives allow photoswitching of immunosuppression. *J. Biol. Chem. 280*, 4842−4850.
(33) Knappe, T. A., Eckert, B., Schaarschmidt, P., Scholz, C., and Schmid, F. X. (2007) Insertion of a chaperone domain converts FKBP12 into a powerful catalyst of protein folding. *J. Mol. Biol. 368*, 1458−1468.
(34) Edlich, F., Weiwad, M., Wildemann, D., Jarczowski, F., Kilka, S., Moutty, M. C., Jahreis, G., Lücke, C., Schmidt, W., Striggow, F., and Fischer, G. (2006) The specific FKBP38 inhibitor N-(N′,N′-dimethylcarboxamidomethyl)cycloheximide has potent neuroprotective and neurotrophic properties in brain ischemia. *J. Biol. Chem. 281*, 14961−14970.
(35) Tradler, T., Stoller, G., Rücknagel, K. P., Schierhorn, A., Rahfeld, J. U., and Fischer, G. (1997) Comparative mutational analysis of peptidyl prolyl *cis/trans* isomerases: active sites of *Escherichia coli* trigger factor and human FKBP12. *FEBS Lett. 407*, 184−190.
(36) Kofron, J. L., Kuzmic, P., Kishore, V., Colón-Bonilla, E., and Rich, D. H. (1991) Determination of kinetic constants for peptidyl prolyl cis-trans isomerases by an improved spectrophotometric assay. *Biochemistry 30*, 6127−6134.
(37) Janowski, B., Wöllner, S., Schutkowski, M., and Fischer, G. (1997) A protease-free assay for peptidyl prolyl *cis/trans* isomerases using standard peptide substrates. *Anal. Biochem. 252*, 299−307.
(38) Mücke, M., and Schmid, F. X. (1994) Folding mechanism of ribonuclease T1 in the absence of the disulfide bonds. *Biochemistry 33*, 14608−14619.
(39) Buchner, J., Grallert, H., and Jakob, U. (1998) Analysis of chaperone function using citrate synthase as nonnative substrate protein. *Methods Enzymol. 290*, 323−338.
(40) Wishart, D. S., Bigam, C. G., Yao, J., Abildgaard, F., Dyson, H. J., Oldfield, E., Markley, J. L., and Sykes, B. D. (1995) ^{1}H, ^{13}C and ^{15}N chemical shift referencing in biomolecular NMR. *J. Biomol. NMR 6*, 135−140.
(41) Herrmann, T., Güntert, P., and Wüthrich, K. (2002) Protein NMR structure determination with automated NOE assignment using the new software CANDID and the torsion angle dynamics algorithm DYANA. *J. Mol. Biol. 319*, 209−227.
(42) Güntert, P., Mumenthaler, C., and Wüthrich, K. (1997) Torsion angle dynamics for NMR structure calculation with the new program DYANA. *J. Mol. Biol. 273*, 283−298.
(43) Güntert, P., Braun, W., and Wüthrich, K. (1991) Efficient computation of three-dimensional protein structures in solution from nuclear magnetic resonance data using the program DIANA and the supporting programs CALIBA, HABAS and GLOMSA. *J. Mol. Biol. 217*, 517−530.
(44) Maestre-Martínez, M., Edlich, F., Jarczowski, F., Weiwad, M., Fischer, G., and Lücke, C. (2006) Solution structure of the FK506-binding domain of human FKBP38. *J. Biomol. NMR 34*, 197−202.
(45) Mulder, F. A., Schipper, D., Bott, R., and Boelens, R. (1999) Altered flexibility in the substrate-binding site of related native and engineered high-alkaline *Bacillus* subtilisins. *J. Mol. Biol. 292*, 111−123.
(46) Li, J., Zoldak, G., Kriehuber, T., Soroka, J., Schmid, F. X., Richter, K., and Buchner, J. (2013) The unique proline-rich domain regulates the chaperone function of AIPL1. *Biochemistry*, DOI: 10.1021/bi301648q.
(47) D'Andrea, L. D., and Regan, L. (2003) TPR proteins: the versatile helix. *Trends Biochem. Sci. 28*, 655−662.

(48) Barent, R. L., Nair, S. C., Carr, D. C., Ruan, Y., Rimerman, R. A., Fulton, J., Zhang, Y., and Smith, D. F. (1998) Analysis of FKBP51/FKBP52 chimeras and mutants for Hsp90 binding and association with progesterone receptor complexes. *Mol. Endocrinol. 12*, 342−354.
(49) Ratajczak, T., and Carrello, A. (1996) Cyclophilin 40 (CyP-40), mapping of its hsp90 binding domain and evidence that FKBP52 competes with CyP-40 for hsp90 binding. *J. Biol. Chem. 271*, 2961−2965.
(50) Cheung-Flynn, J., Roberts, P. J., Riggs, D. L., and Smith, D. F. (2003) C-terminal sequences outside the tetratricopeptide repeat domain of FKBP51 and FKBP52 cause differential binding to Hsp90. *J. Biol. Chem. 278*, 17388−17394.